Journal of Ethnopharmacology 270 (2021) 113816

Contents lists available at ScienceDirect

Journal of Ethnopharmacology

journal homepage: www.elsevier.com/locate/jethpharm

Network pharmacology-based mechanism prediction and pharmacological validation of Xiaoyan Lidan formula on attenuating alpha-naphthylisothiocyanate induced cholestatic hepatic injury in rats

Meiqi Wang, Fangle Liu, Yufeng Yao, Qiuyu Zhang, Zenghui Lu, Runjing Zhang, Changhui Liu, Chaozhan Lin **, Chenchen Zhu *

School of Pharmaceutical Sciences, Guangzhou University of Chinese Medicine, No.232 Waihuandong Rd, Guangzhou Higher Education Mega Center, Guangzhou, 510006, China

ARTICLE INFO

Keywords:
XYLDF
Network pharmacology
Cholestatic hepatic injury
Inflammation
FXR
NF-κB

ABSTRACT

Ethnopharmacological relevance: The well-known Chinese prescription, Xiaoyan Lidan Formula (XYLDF), possesses efficiency of heat-clearing, dampness-eliminating and jaundice-removing. It has long been used clinically for the treatment of hepatobiliary diseases due to intrahepatic cholestasis (IHC). However, the mechanism of XYLDF for its therapeutic effects remains elusive.

Aim of the study: The study aimed to explore the potential targets for liver protective mechanism of XYLDF based on network pharmacology and experimental assays in ANIT-induced cholestatic hepatic injury (CHI) in rats.

Materials and methods: On the basis of the 29 serum migrant compounds of XYLDF elucidated by UPLC-TOF-MS/MS, a network pharmacology approach was applied for the mechanism prediction. Systematic networks were constructed to identify potential molecular targets, biological processes, and signaling pathways. And the interactions between significantly potential targets and active compounds were simulated by molecular docking. For the mechanism validation, an ANIT-induced rat model was used to evaluate the effects of XYLDF on CHI according to serum biochemistry, bile flow rates, histopathological examination, and the gene and protein expression including enzymes related to synthesis, export, and import of bile acid in liver and ileum, and those of inflammatory cytokines, analyzed by RT-qPCR and WB.

Results: The results of network pharmacology research indicated TNF (TNF-α), RELA (NF-κB), NR1H4 (FXR), and ICAM1 (ICAM-1) to be the important potential targets of XYLDF for cholestatic liver injury, which are related to bile metabolism and NF-κB-mediated inflammatory signaling. And the molecular docking had pre-validated the prediction of network pharmacology, as the core active compounds of XYLDF had shown strong simulation binding affinity with FXR, followed by NF-κB, TNF-α, and ICAM-1. Meanwhile, the effects of XYLDF after oral administration on ANIT-induced CHI in rats exhibited the decreased levels of transaminases (ALT and AST), TBA, and TBIL in serum, raised bile flow rates, and markedly improved hepatic histopathology. Furthermore, consistent to the above targets prediction and molecular docking, XYLDF significantly up-regulated the expression of FXR, SHP, BSEP, and MRP2, and down-regulated CYP7A1 and NTCP in liver, and promoted expression of IBABP and OSTα/β in ileum, suggesting the activation of FXR-mediated pathway referring to bile acid synthesis, transportation, and reabsorption. Moreover, the lower levels of TNF-α in plasma and liver, as well as the reduced hepatic gene and protein expression of NF-κB, TNF-α, and ICAM-1 after XYLDF treatment revealed

Abbreviations: XYLDF, Xiaoyan Lidan Formula; Intrahepatic Cholestasis, IHC; Cholestatic Hepatic Injury, CHI; KEGG, Kyoto Encyclopedia of Genes and Genomes; TBA, total bile acid; TBIL, total bilirubin; ALT, alanine aminotransferase; ANIT, alpha-naphthylisothiocyanate; AST, aspartate transaminase; FXR, Farnesoid X receptor; SHP, small heterodimer partner; NF-κB, nuclear factor kappa-B; IκBα, inhibitory kappa-B alpha; p-IκBα, phosphorylated inhibitory kappa-B alpha; TNF-α, tumor necrosis factor α; ICAM-1, intercellular cell adhesion molecule-1; qRT-PCR, Quantitive Real Time-polymerase chain reaction; WB, western blot.

* Corresponding author. Department of Phytochemistry, School of Pharmaceutical Sciences, Guangzhou University of Chinese Medicine, No.232 Waihuandong Rd, Guangzhou Higher Education Mega Center, Guangzhou, 510006, China.

** Corresponding author. Department of Phytochemistry, School of Pharmaceutical Sciences, Guangzhou University of Chinese Medicine, No.232 Waihuandong Rd, Guangzhou Higher Education Mega Center, Guangzhou, 510006, China.

E-mail addresses: linchaozhan@gzucm.edu.cn (C. Lin), zhucc@gzucm.edu.cn (C. Zhu).

https://doi.org/10.1016/j.jep.2021.113816
Received 24 February 2020; Received in revised form 4 January 2021; Accepted 6 January 2021
Available online 12 January 2021

the suppression of NF-κB-mediated inflammatory signaling pathway, as evidenced by the inhibition of nuclear translocation of NF-κB.
Conclusions: XYLDF exhibited an ameliorative liver protective effect on ANIT-induced cholestatic hepatic injury. The present study has confirmed its mechanism as activating the FXR-regulated bile acid pathway and inhibiting inflammation via the NF-κB signaling pathway.

1. Introduction

Cholestatic hepatic injury (CHI) is frequently occurring mostly due to intrahepatic cholestasis (IHC), a clinic syndrome with systemic circulation and intrahepatic accumulation of excessive toxic bile acids (Hirschfield et al., 2013). Though the etiology of IHC is complicated, this syndrome induced by any cause can interrupt bile acids metabolic and induce retention of toxic substances, such as bile acids, leading to cholestatic hepatobiliary disease (Carbone and Neuberger, 2014). Bile acid synthesis and transport disorder in the hepatobiliary system is considered as an essential risk to induce CHI (Li et al., 2017). As revealed by researches on CHI, alpha-naphthylisothiocyanate (ANIT) is a hepatotoxicant, which injures bile duct epithelium and leads to cholestasis (Palmeira et al., 2003). Therefore, an ANIT-induced cholestatic liver injury model in rats is commonly used for modeling human cholestatic hepatitis (Mohi-Ud-Din and Lewis, 2004; Zhao et al., 2015). It has been illustrated that nuclear receptors and transcription factors, such as Farnesoid X receptor (FXR), can regulate bile acid transporters and enzymes in ANIT-induced CHI rats (J.G. Marin et al., 2015). FXR plays a critical regulatory role on enterohepatic circulation of bile acid through depressing synthesize and reabsorption, and increasing efflux, transportation and metabolism of bile acid (Cui et al., 2009). In clinic, ursodeoxycholic acid (UDCA) is recommended for most patients with cholestatic hepatitis as first choice therapy (Fickert et al., 2013), but a certain number of patients present limited response to this therapy and eventually progress to cirrhosis and liver failure (Ou et al., 2016). Therefore, the development of effective drug for cholestatic hepatitis is still urgently needed.

Traditional Chinese Medicine (TCM) plays an active role in the treatment of liver diseases with safety and efficacy (Zhang et al., 2019; Zhu and Feng, 2019). Xiaoyan Lidan Formula (XYLDF), consisted of three Chinese herbal medicines as Herba andrographis (dried herb of *Andrographis paniculata* (Burm.f.) Nees, *Chuanxinlian*), Herba rabdosia (dried herb of *Rabdosia serra* (Maxim.) Hara, *Xihuangcao*) and Ramulus et folium picrasmae (dried twigs and leaves of *Picrasma quassioides* (D. Don) Benn, *Kumu*), possesses the efficiency of clearing heat, eliminating dampness, removing jaundice and reducing inflammation (Yang et al., 2016; Shen et al., 2018; Tang et al., 2014). It has long been used for the treatment of cholestasis related hepatobiliary disease, such as cholestatic hepatitis, cholecystitis, cholangitis and hepatolithiasis (Chinese Pharmacopoeia Commission, 2020). Our previous studies have revealed that XYLDF improved ANIT-induced CHI in rats (Liu et al., 2016), and its mechanism was involved in the turbulence of multiple metabolic pathways, especially the primary bile acid metabolism pathway as revealed by targeted and non-targeted metabolomics (Zhang et al., 2019). However, the precise molecular mechanism of XYLDF on CHI remains mostly unknown and needs to be elucidated.

Considering that XYLDF has the characters of multi-component and multi-target, network pharmacology, combined with pharmacodynamics, could be regarded as a novel strategy to address the complexity of the molecular mechanism of XYLDF (Liang et al., 2014; Banerjee et al., 2019). The approach of network pharmacology is widely used in the mechanism research of herbal medicines and TCM formulas based on multiple networks of herbs-targets-disease-protein, realizing the prediction of drug targets for improving drug efficiency (Liu and Du, 2010; Zhang et al., 2015). However, the prediction of molecular mechanisms of TCM using network pharmacology was mostly from literature without experimental validation, which might lead to unreliable results. Therefore, pharmacological experiments following the prediction are necessary for the confirmation of its accuracy.

Given that the pharmacological mechanism of XYLDF in the treatment of cholestatic liver injury remains unclear, the use of combined network pharmacology approach and experimental validation might be a strategy to explore the underlying mechanism of XYLDF on CHI. Here we firstly applied network pharmacology to screen the possible molecular targets and signaling pathways of XYLDF. Next, we further validated these targets and pathways by molecular docking and pharmacological assay in ANIT-induced liver injury rats after XYLDF treatment by analyzing a series of mRNA and protein levels. The activation on the FXR-mediated bile acid pathway of XYLDF and its anti-inflammation effect based on the NF-κB signaling pathway was observed in this study.

2. Materials and methods

2.1. Chemicals and reagents

ANIT (Lot NO. F1707046) and medical-grade soybean oil (Lot NO. F1613059) were purchased from Aladdin Company. UDCA (Lot NO. 15C09094L) was supplied by Dr. Falk Pharma GmbH. Alanine aminotransferase (ALT), aspartate aminotransferase (AST), total bile acids (TBA), and total bilirubin (TBIL) kits were supplied by Nanjing Jiancheng Institute of Biotechnology (Nanjing, China). All biochemical indicator kits and other chemicals were commercially available. UPLC-MS chromatography-grade Acetonitrile and methanol were purchased from Fisher Chemical Company (Geel, Belgium). Formic acid was purchased from Sigma-Aldrich. Ultrapure water was purified by a Millipore water purification system (Millipore, Billerica, MA, USA) for the preparation of samples and buffer solutions.

2.2. Materials and dose design of XYLDF

The plant material was identified and confirmed. Dried aboveground parts of *R. serra* (**Xihuangcao**) and *A. paniculata* (**Chuanxinlian**) were collected from Guangdong province. Dried branches and leaves of *P. quassioides* (**Kumu**) were purchased from Hubei province. The above samples were identified by Prof. Chaomei Pan (Department of Botany, Guangzhou University of Chinese Medicine). The voucher specimens were deposited in School of Pharmaceutical Sciences, Guangzhou University of Chinese Medicine (Guangzhou, China).

The XYLDF sample was prepared and quality controlled according to our previous study (Zhang et al., 2019). The daily dose of XYLDF, 46.8 g (expressed by quantity of crud drugs) in clinic, was applied for the medium dose, 5 g/kg (calculated according to the dosage conversion coefficient of humans and rats) for the present study. And the doubled and half of the medium dose were applied for high (10 g/kg) and low doses (2.5 g/kg) accordingly (Chinese Pharmacopoeia Commission, 2020; Chen and Zhang, 2016). The dosage regimen of all groups was illustrated in our previous research (Zhang et al., 2019). The diagram of the animal experiment design was shown in Fig.S10.

2.3. Animals and experimental groups

Male SD rats (220 ± 20 g) were obtained from the Experimental Animal Center of Guangzhou University of Chinese Medicine (Guangzhou, China; with license No. of SCXK, 2013-0034). Animals'

maintenance and treatment protocols were in accordance with the Animal Ethics Committee of Guangzhou University of Chinese Medicine (Guangzhou, China) for the care and use of laboratory animals. International rules were strictly followed in handling the animals.

For serum medicinal chemistry study, eight rats were orally administrated with XYLDF (5 g/kg) for 7 days. For the pharmacological study, forty-eight rats were acclimated for one week in quarantine then randomly divided into six groups on average, as normal control group, ANIT-induced model group, UDCA-treated positive group, and three XYLDF-treated groups with high (10 g/kg), medium (5 g/kg) and low dosages (2.5 g/kg).

2.4. Serum migrant compounds analysis of XYLDF based on UPLC-Q-TOF-MS

2.4.1. Sample collection and preparation

The serum samples were taken from the angular vein of the rats on the 7th day, after the administration of XYLDF at 5min, 15min, 30min, 1 h, 1.5 h, 2 h, 3 h, 5 h, 7 h, 9 h, and 12 h. The serum samples of each rat from the above time points were mixed, concentrated, and redissolved with methanol. The supernatant was stored at −20 °C before analysis.

2.4.2. UHPLC-Q-TOF-MS/MS analysis

UPLC analyses were performed on a Shimadzu UPLC system (Nexera UHPLC LC-30 A, Japan). Samples were separated on an Acquity BEH C18 column (2.1 mm × 100 mm, 1.7 μm). The mobile phase consisted of acetonitrile (A) and water containing 0.1% formic acid (B). Mass spectrometry was conducted on an AB SCIEX Triple TOF™ 5600+ (Foster City, CA, USA). The data were acquired using Analyst®TF 1.7 software (AB Sciex, Foster City, CA, USA).

2.5. Network pharmacology-based mechanism prediction of XYLDF on CHI

2.5.1. Screening of therapeutic targets of active components related to CHI

Based on the serum chemical study of XYLDF by UHPLC-Q-TOF-MS/MS, the serum migrant compounds were considered as active compounds. On the basis of those identified compounds, several online databases were employed to predict the possible treatment targets. First of all, SMILES strings and 3D molecular structures of the compounds were acquired from PubChem (https://pubchem.ncbi.nlm.nih.gov/), an official chemical database which contains comprehensive chemical information. Then, the SMILES strings were imported into TCMSP (http://lsp.nwu.edu.cn/tcmsp.php), Swiss Target Prediction (http://www.swisstargetprediction.ch/), and STITCH database (http://stitch.embl.de/) to search for potential targets of the compounds. Then the related genes were standardized and screened for Homo sapiens by the Retrieve/ID mapping tool in the UniProt database (https://www.uniprot.org/uploadlists/). Secondly, the obtained targets were further filtered according to their pertinence with CHI. "Cholestasis", "cholestatic hepatic injury" and "cholestatic liver injury" were inputted as keywords in the database, including OMIM (https://omim.org/), TTD (http://bidd.nus.edu.sg/group/ttd/) and GeneCards (http://www.genecards.org/), to search for disease targets. Targets with relevance score and inference score over 35 were highlighted. Finally, the targets of compounds were mapped to the targets of disease to screen out therapeutic targets of XYLDF on CHI.

On the basis of therapeutic targets of XYLDF on CHI, gene names were uploaded onto the String Database (https://string-db.org) to obtain protein-protein interaction (PPI) data and to explore the interaction between those proteins.

2.5.2. Network construction and analysis

In this study, to determine a systematic understanding of the complex relationships among compounds, targets, and diseases, a network visualization software, Cytoscape (http://cytoscape.org/, ver. 3.2.1), was used to build the networks. The selected targets and data were input into Cytoscape to construct the following three networks, i.e., compound-compound target (C–C) network, compound-therapeutic target (C-T) network, and PPI network of cholestatic hepatic injury related targets in XYLDF. The PPI network was constructed using Cytoscape by importing the data of node1, node2, and combined score in the TSV document from the String database.

2.5.3. Pathway enrichment and functional prediction

To further mining the potential function of XYLDF on CHI, KEGG Pathway and Gene Ontology (GO) enrichment were analyzed via ClueGo, which is a comprehensive set of gene functional annotation tools for the investigation of biological function and mechanisms possessed by large lists of genes. The cluster of KEGG Pathway Analysis was set to 4, the Kappascore was 0.45, and the percent of Genes was 5%. In the GO enrichment analysis, the GO term "biological process" was highlighted. The cluster of GO biological process enrichment analysis was set to 3, the Kappascore was 0.4, the percent of Genes was 10%, and the level was 3–5.

2.5.4. Molecular docking

In this study, targets and active compounds with a high degree in the network were selected, and the possible compound-target interaction was further predicted based on the protein-ligand complexes in crystal structures. Structure information of the ligand molecules was obtained from the NBCI PubChem database (https://pubmed.ncbi.nlm.nih.gov/). The 3D structures of the ligands were built and optimized by Chem3D (ChemDraw software 17.0), and saved as Mol2 format. The protein crystal structure of the targets was obtained from RCSB Protein Data Bank (PDB, https://www.rcsb.org/). The water and ligand molecules were removed from the protein crystal structure. Then proteins and ligands were optimized by Autodock Tools 4.2.6 and saved as PDBQT files. The docking process was performed by AutoDock 4 to analyze the binding properties of the ligands for each protein. Proteins with lower binding energy were considered as potential targets of XYLDF in the treatment of IHC liver injury. And the top three ligands with the lowest binding energy were selected for binding mode analysis.

2.6. Pharmacological validation of XYLDF on CHI

2.6.1. Bile flow rate analysis

One hour after administration on the last day of the experiment, the rats received cystic duct incubation under anesthesia at 37 °C. The bile specimens were collected at half-hour intervals into pre-weighed polyethylene tubes for 1.5 h. The bile flow rate was calculated by the weight of each specimen as body weight using the following equation:

$$\textbf{Bile flow rate}\ (\mu L/min/100\ g\ body\ weight) = \frac{(\boldsymbol{m_2}-\boldsymbol{m_1})\times 10^5}{\mathbf{M}\times 30}$$

$\mathbf{m_1}$ represents weight (mg) of the polyethylene, and $\mathbf{m_2}$ represents weight (mg) of polyethylene with bile specimen, and $\mathbf{M}$ represents body weight (g) of the rat. And the density of bile is 1 g mL^{-1} (Crocenzi et al., 2001). The bile specimens were collected every 30 min.

2.6.2. Serum biochemical indicator

The blood of each rat was taken via abdominal aorta after the bile acid collection. The serum was obtained by centrifugation, and contents of ALT, AST, TBA, and TBIL in the serum were measured.

2.6.3. Histopathology

Hepatic tissues were fixed with 10% neutral buffered formalin, embedded in paraffin, sectioned at 5 μm, and stained with hematoxylin and eosin (HE) for histopathological examination. The histological sections were examined by optical microscopy.

2.6.4. Inflammatory cytokine quantification

Levels of TNF-α in plasma and liver homogenate were measured

using ELISA kits (Meimian, Jiangsu, China). Hepatic tissues were homogenized in ice-cold normal saline and then centrifuged at 12,000×*g* under 4 °C for 15 min. The supernatants were collected and the protein concentrations were determined by BCA protein assays (Guangzhou Dingguo biology, Guangzhou, China).

2.6.5. Western blot analysis

Liver and ileum tissues were minced and homogenized in ice-cold RIPA lysis buffer with 1% PMSF, and protein concentration was detected by BCA protein assay. Total proteins were separated by electrophoresis on 12% sodium dodecyl sulfate-poly-acrylamide minigels (SDS-PAGE), and electro-transferred onto a polyvinylidence difluoride (PVDF) membrane. After blocking with 5% nonfat dry milk in Tris-buffered saline for 2 h at room temperature, membranes were incubated overnight at 4 °C with antibodies, primary antibodies against FXR, SHP, MRP2, IBABP, NF-κB, IκBα, p-IκBα, TNF-α, ICAM1 and Lamin B1 were purchased from Abcam (Cambridge, UK); NTCP was provided by Thermo Fisher (Rockford, USA); OSTα and OSTβ were supplied by Beijing Biosynthesis Biotechnology CO., LTD. (Beijing, China). After washed with TBST for three times, the membranes were incubated with the horseradish peroxidase-conjugated secondary antibody (1:3000) and washed as the above, then detected by a western blotting detection system. Grey intensity of protein bands was analyzed and quantified by Image Lab.

2.6.6. Real-time quantitative polymerase chain reaction (RT-qPCR)

Total RNA was extracted from liver and ileum using the RNA Extraction Kit (EZgene™ Biozol RNA extraction kit, Biomiga, Inc, San Diego, USA). The purity and concentration of RNA were evaluated using a NANODROP 2000 spectrophotometer (Thermo Scientific, USA). RNA was reverse-transcribed into cDNA by using Bestar™ qPCR RT Kit (DBI Bioscience, Germany). Quantitative real-time PCR was performed using Bestar® SybrGreen qPCR Mastermix (DBI Bioscience, Germany) and Applied Biosystems StepOne™ Real-Time PCR system (Thermo Fisher Scientific, USA). The quantity of mRNA was normalized with an internal standard rat GAPDH. Gene-specific rat primers used are: GAPDH forward primer (5′-CAAGGATACTGAGAGCAAGAGA-3′) and reverse primer (5′-AGGCCCCTCCTGTTGTTAT-3′); FXR forward primer (5'-GACCACGAAGACCAGATTGC -3′) and reverse primer (5'-GAGATGCCGCTCTTTCGAAT-3′); SHP forward primer (5'-CGCATACCTGAAAGGCACTA -3′) and reverse primer (5'-AGGGCGGAAGAAGAGATCTA -3′); BSEP forward primer (5'-CAACGCATTGCTATTGCTCG -3′) and reverse primer (5'-GTTCTGGATGGTGGACAAACG-3′); MRP2 forward primer (5'-GTTGGCTCACCTCAGATCCT -3′) and reverse primer (5'-GAGGCTATCCGTCTCGAGAT-3′); NTCP forward primer (5'-GCTTAGCATCATCCTGGTGTT -3′) and reverse primer (5'-CACAAGTGAGCCTTGATCTTG-3′); IBABP forward primer (5'-CTTACTCTGGGGGCAACATC -3′) and reverse primer (5'-ACGGTTGCCTTGAACTTCTT-3′); OSTα forward primer (5'-CGCTTGCTCACCTCCCTATT -3′) and reverse primer (5'-GGCGGTAAACAAGCCTCATA -3′); OSTβ forward primer (5'-TTTCCGTTCAGAGGATGCAA -3′) and reverse primer (5'-GTCTTCTGGCATTCCGTTGT-3′); NF-κB forward primer (5'-GACGATCTGTTTCCCCTCAT -3′) and reverse primer (5'-GCTTCTCTCCCCAGGAATAC-3′); TNF-α forward primer (5'-GAAACACACGAGACGCTGAA -3′) and reverse primer (5'-CCACTCAGGCATCGACATTC-3′); ICAM-1 forward primer (5'-CTTTAGCAGCTCAACAATGG 3′) and reverse primer (5'-CATTTTCTCCCAGGCATTC-3').

2.7. Statistical analysis

All the presented data were confirmed in at least three independent experiments and were presented as means ± SD. Comparisons between multiple groups were performed using one-way ANOVA with LSD's test by SPSS 19.0 software. The statistical significance of differences between mean values was calculated using the non-paired *t*-test. *P* values less than 0.05 were considered to be statistically significant.

3. Results

3.1. Identification of serum migrant compounds of XYLDF based on UPLC-Q-TOF-MS

The serum samples of rats administrated with XYLDF were analyzed by UPLC-Q-TOF-MS in both positive and negative ion modes. The data were analyzed with MasterViwe mode of PeakView 2.0 (AB SCIEX, Milwaukee, USA) and total ion chromatogram (TIC) was acquired (Fig. S1). The components absorbed into the blood were identified with the combination of additional literature. A total of 29 serum migrant compounds (Table S1) were detected from the serum samples in light of the typical fragment ions and structural characteristics (Fig. S2), including 6 components were from *Xihuangcao* (XHC), 9 from *Chuanxinlian* (CXL) and 14 from *Kumu* (KM) (Table S2).

3.2. Potential targets screening of XYLDF by network pharmacology

The C–C network is a preliminary observation of the relationship between active compounds and compound targets. In this study, 29 compound nodes and 401 compound target nodes were included in the constructed C–C network (Fig. S3). It suggested the characteristics of multi-component and multi-target of XYLDF. For the prediction of key compounds for the treatment of CHI by XYLDF, a C-T network was performed based on target mapping between compound targets and therapeutic targets. In our C-T network, 29 compounds and 42 therapeutic targets were finally selected (Fig. 1). The compounds with high degree value over 5 were considered as potential vital active components (Table S4). Meanwhile, the top 5 therapeutic targets exhibiting high degree value were AKR1B10, CHEK1, PTGS1, PARP1 and TNF (Table S4). The result indicated that multiple compounds and targets were highly related to the development of the disease.

However, further data mining is necessary for exploring deeper interaction between targets. Therefore, a PPI network was constructed to reveal the underlying relationships between targets (proteins) of XYLDF. As the bigger node size and darker red color reflected a higher degree value, the big node TNF with conspicuous red was focused (Fig. 2). The network also indicated that the top 5 targets with a higher degree were TNF, RELA (NF-κB), NR1H4 (FXR), ICAM-1, and CYP1A1 (Table 1), which could be considered as vital targets in the pharmacological mechanisms of XYLDF.

3.3. KEGG pathway enrichment and GO biological process prediction

The GO biological process and KEGG Pathway enrichment were carried out by ClueGO function module of Cytoscape to identify relevant pathways and functions. The KEGG pathway enrichment results demonstrated that the bile secretion pathway, NF-kappa B signaling pathway, and TNF signaling pathway were enriched (Fig. 3A, Table 2), which were associated with the bile acid metabolism and inflammatory process. Moreover, GO biological process analysis data revealed that the putative targets modulated complicated bioprocess including bile acid and bile salt transport, reactive oxygen species (ROS) biosynthetic process, steroid biosynthetic and metabolic process, and liver regeneration (Fig. 3 B, Table 3), suggesting that the potential mechanism of XYLDF on CHI might be relevant to the regulation effects of anti-inflammation and bile acid signaling pathway. Of note, The PPI network showed that RELA(NF-κB), NR1H4 (FXR), and ICAM1 had a high degree among the 41 targets.

Considered that FXR, a bile acid receptor, is associated with bile acid homeostasis by the regulation of bile acid synthesis and transport (Wagner et al., 2009), and NF-κB is a master transcriptional regulation of

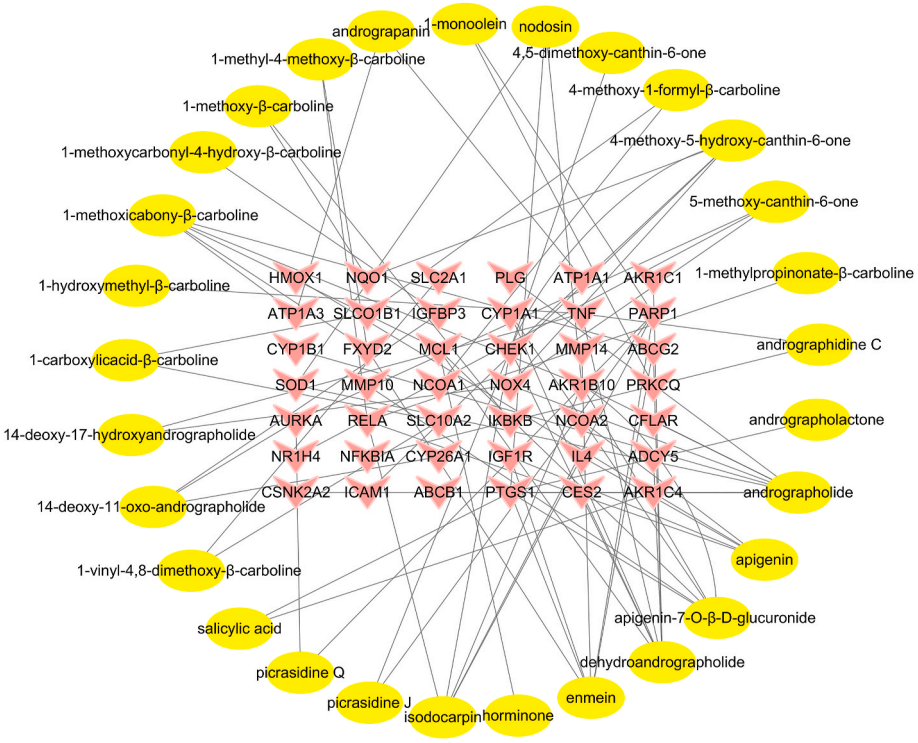

Fig. 1. Effective compounds-CHI targets network of XYLDF. The yellow circles represented the compounds in XYLDF, and the red "V" arrows represented the screened therapeutic targets. (For interpretation of the references to color in this figure legend, the reader is referred to the Web version of this article.)

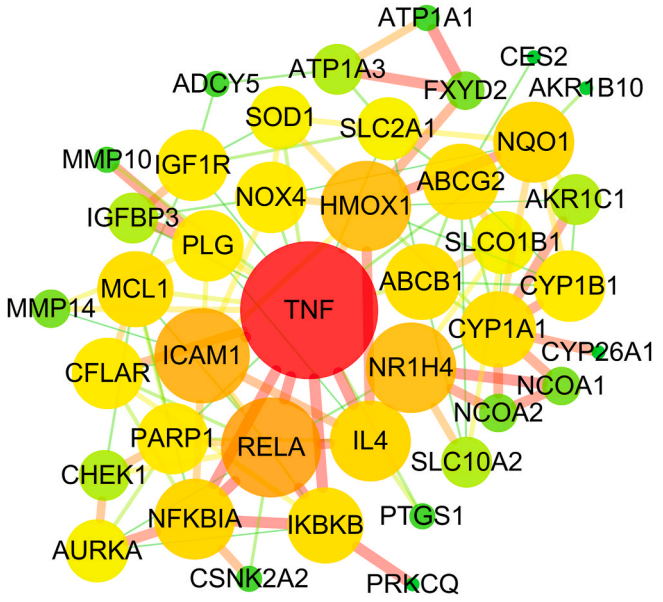

Fig. 2. Protein-protein interactions (PPI) network of XYLDF. A bigger node size meant a higher value. With the increasing degree value, the node turned from green to red. The thickness of the edge reflected the value of the combined score, and a thicker line represented a higher score. (For interpretation of the references to color in this figure legend, the reader is referred to the Web version of this article.)

pro-inflammatory genes (Donepudi et al., 2012), we, therefore, speculate that the hepatoprotective mechanism of XYLDF might be related to the FXR-regulated bile acid pathway and NF-κB-mediated pro-inflammatory process, which are the two crucial pathogenic factors of CHI.

3.4. Molecular docking

Molecular docking study provides a rational analysis for the interactions between significant active compounds and potential protein targets, which can explore effective targets of XYLDF with higher tendency and accuracy. Since the results of network pharmacology research indicated TNF (TNF-α), RELA (NF-κB), NR1H4 (FXR), and ICAM1 (ICAM-1) to be the important potential targets, these four targets with high degree from PPI network were selected for molecular docking. The docking simulation results of eight significant active compounds, which had high degree in the compound-target network, were showed in Table 4. Lower docking energy indicating a stronger binding affinity and higher docking score. The results showed that TNF, NF-κB, FXR, and ICAM-1 all had good binding energy. Isodocarpin tended to have the best affinity towards the studied targeted proteins according to the docking energy, suggesting that isodocarpin might be a significant compound in XYLDF with potential bioactivity. Furthermore, the small molecule ligands showed the best activity when docking with FXR. NF-κB, TNF-α and ICAM-1 was also showed good docking affinity with the ligands. The docking energy of isodocarpin with FXR was −9.08, which was the lowest one, nodosin was −8.79, and andrographolide was 8.28. As shown in Fig. 4, isodocarpin (Fig. 4A), nodosin (Fig. 4C) and andrographolide (Fig. 4E) buried in the binding pocket of the FXR protein formed by amino-acid residues based on the hydrogen and hydrophobic interactions. Among these residues, isodocarpin had hydrophobic bonding with LEUA:291, ILEA:356, META:294, LEUA:352, ILEA:339, and ALAA:295 in different directions (Fig. 4B). Meanwhile, the hydrogen-bond interactions between nodosin and FXR were formed by META:294, LEUA:291, and LALA:295 (Fig. 4D). As to andrographolide, the hydroxy had a hydrogen bonding with SERA:336, while the hydrogen bonds were formed with META:369, ILEA:361, ILEA:356, LEUA:291, META:294 and LEUA:352 (Fig. 4F). The results of the molecular docking simulation above pre-validated TNF, NF-κB, FXR, and ICAM1 as potential targets of XYLDF, while FXR tended to be the most effective targets. Consistently, isodocarpin and 1-methoxicabony-

Table 1
Information of potential anti-CHI targets (degree>1) of XYLDF.

NO.	Uniprot ID	Gene	Targets	Degree
1	P01375	TNF	Tumor necrosis factor	20
2	Q04206	RELA	Nuclear factor NF-kappa-B p65 subunit	12
3	Q96RI1	NR1H4	Bile acid receptor	11
4	P05362	ICAM1	Intercellular adhesion molecule 1	10
5	P04798	CYP1A1	Cytochrome P450 1A1	10
6	P25963	NFKBIA	NF-kappa-B inhibitor alpha	8
7	P09601	HMOX1	Heme oxygenase 1	8
8	P05112	IL4	Interleukin-4	8
9	O14920	IKBKB	Inhibitor of nuclear factor kappa-B kinase subunit beta	7
10	P09874	PARP1	Poly [ADP-ribose] polymerase 1	7
11	P15559	NQO1	NAD(P)H dehydrogenase [quinone] 1	7
12	O15519	CFLAR	CASP8 and FADD-like apoptosis regulator	7
13	P08069	IGF1R	Insulin-like growth factor 1 receptor	7
14	P08183	ABCB1	P-glycoprotein 1	6
15	P00747	PLG	Plasminogen	6
16	Q9UNQ0	ABCG2	ATP-binding cassette sub-family G member 2	6
17	Q07820	MCL1	Induced myeloid leukemia cell differentiation protein Mcl-1	6
18	Q16678	CYP1B1	Cytochrome P450 1B1	6
19	Q9Y6L6	SLCO1B1	Solute carrier organic anion transporter family member 1B1	6
20	Q9NPH5	NOX4	NADPH oxidase 4	5
21	Q15788	NCOA1	Nuclear receptor coactivator 1	5
22	P17936	IGFBP3	Insulin-like growth factor-binding protein 3	5
23	O14965	AURKA	Aurora kinase A	5
24	Q12908	SLC10A2	Ileal sodium/bile acid cotransporter	4
25	P00441	SOD1	Superoxide dismutase [Cu–Zn]	4
26	P11166	SLC2A1	Solute carrier family 2, facilitated glucose transporter member 1	4
27	P13637	ATP1A3	Sodium/potassium-transporting ATPase subunit alpha-3	4
28	Q98TW1	NCOA2	Nuclear receptor coactivator 2	4
29	Q04828	AKR1C1	Aldo-keto reductase family 1 member C1	3
30	O14757	CHEK1	Serine/threonine-protein kinase Chk1	3
31	O95622	ADCY5	Adenylate cyclase type 5	3
32	P50281	MMP14	Matrix metalloproteinase-14	3
33	P54710	FXYD2	Sodium/potassium-transporting ATPase subunit gamma	2
34	P09238	MMP10	Stromelysin-2	2
35	O14965	ATP1A1	Aurora kinase A	2
36	Q04759	PRKCQ	Q04759	2
37	P19784	CSNK2A2	Casein kinase II subunit alpha'	2
38	P23219	PTGS1	Prostaglandin G/H synthase 1	1
39	O43174	CYP26A1	Cytochrome P450 26A1	1
40	O60218	AKR1B10	Aldo-keto reductase family 1 member B10	1
41	O00748	CES2	Cocaine esterase	1

β-carboline exhibited certain activity of inducing FXR in the reporter assay (Fig. S9). It suggested that XYLDF might exert protective effects against cholestic liver injury through modulating FXR activities.

3.5. Validation of potential therapeutic mechanism of XYLDF

3.5.1. Hepatoprotective activity of XYLDF against ANIT-induced CHI in rats

The anti-CHI effect of XYLDF was demonstrated in an ANIT-induced cholestatic hepatic injury in rats. The bile flow played a vital role in ANIT-induced CHI. Fig. 5C showed that the bile flow rate was significantly ($p < 0.01$) reduced in model group, compared to that in the control group. As the disrupted bile flow in the cholestasis leads to toxic bile acid accumulation and liver damage, the recovery of continuous bile flow is essential in the treatment of cholestatic liver injury. In this study, the bile flow rate was increased at the dose of 5 g/kg and 2.5 g/kg, generally increased in 10 g/kg group, slightly increased in the UDCA group, which means the cholestasis was alleviated. Meanwhile, biochemical indicators of hepatic damage and CHI in control, model, UDCA, and XYLDF (2.5 g/kg, 5 g/kg, and 10 g/kg) groups were determined. Comparing with the control group, levels of ALT, AST, TBA, and TBIL in serum were increased in the model group (Fig. 5A and B). Besides, XYLDF ameliorated ANIT-induced ALT, AST and TBA incensement to exhibit a protective effect, indicating that the hepatic injury was improved.

Hepatic histopathologic analysis from ANIT-treated rats exhibited characteristic pathological lesions, such as infiltration of inflammatory cells and large areas of cholangitis with marked bile duct proliferation (Fig. 5D). In contrast, XYLDF evidenced mitigated pathological changes, including smaller areas of cholangitis, less inflammatory cell infiltration, and less bile duct proliferation. These results suggested that XYLDF protected the liver against ANIT-induced cholestatic hepatic injury in rats.

3.5.2. XYLDF regulated FXR-mediated bile acid pathway to alleviate CHI

Comprehensively considering the potential targets of XYLDF on FXR-bile acid signaling from network pharmacology, and the significant role of FXR plays in the bile acid secretion pathway and inflammation pathway (Chávez-Talavera et al., 2017), especially in ANIT-induced CHI (Meng et al., 2015), the effects of XYLDF on FXR-regulated bile acid signaling were therefore evaluated. The relative mRNA expression of FXR, SHP, BSEP, MRP2 (Fig. 6A) in the liver, as well as the relative mRNA expression of IBABP, OSTα and OSTβ (Fig. 6B) in ileum were significantly up-regulated by XYLDF, while CYP7A1 and NTCP (Fig. 6A) were remarkably down-regulated. The results of protein expression of FXR, SHP, MRP2, NTCP, IBABP, OSTα, and OSTβ (Fig. 6C–F) had the same trend as those of mRNA. These experimental data were in accordance with the results of network pharmacology research. And it suggested that XYLDF regulated the FXR-mediated bile acid signaling pathway, which could promote the inhibition of bile acid synthesis, and re-uptake of bile acid and its transportation, and consequent, to improve ANIT-induced cholestatic hepatic injury.

3.5.3. XYLDF suppressed inflammation and inhibited NF-κB nuclear translocation

Furthermore, network pharmacology also demonstrated the correlation between XYLDF and NF-κB, a crucial modulator on inflammation and oxidative stress in cholestatic liver disease (El Kasmi et al., 2018; Zhang et al., 2018). In our study, ANIT led to a significant increase of TNF-α level in plasma and liver tissue in rats with cholestatic hepatic injury, compared with those in the control group. And the decreased level of TNF-α in XYLDF group indicated the inflammation response was relieved. (Fig. 7A). Meanwhile, ANIT administration also activated NF-κB in mRNA level and induced the expression of TNF-α and ICAM-1 (Fig. 7B–D). With the treatment of XYLDF, the abnormal expression of NF-κB and the above cytokines by ANIT was decreased remarkably (Fig. 7B–D), which indicated that the anti-inflammation effect of XYLDF was highly correlative with NF-κB activation.

To further validate the inhibition of XYLDF to the NF-κB signaling pathway, the protein expression of IκBα, p-IκBα and NF-κB in both cytoplasm and nucleus was measured. The result showed that IκBα was decreased in the model group, and large amount IκBα was phosphorylated into p-IκBα (Fig. 7E and F). After oral administration of XYLDF, the protein level of IκBα was raised, and that of p-IκBα was reduced(Fig. 7E and F), which indicated the inhibition of phosphorylation of IκBα. Meanwhile, the raised NF-κB protein levels in the nucleus induced by ANIT were significantly lowered in XYLDF group, as well as the protein levels in the cytoplasm were elevated (Fig. 7G and H). As the nuclear translocation of NF-κB (from the cytoplasm into the nucleus) is the sign of NF-κB signaling pathway activation (Martincuks et al., 2017), it indicated that the atcivation of NF-κB was inhibited by XYLDF. The above results evidently suggested that XYLDF had an inhibition effect on

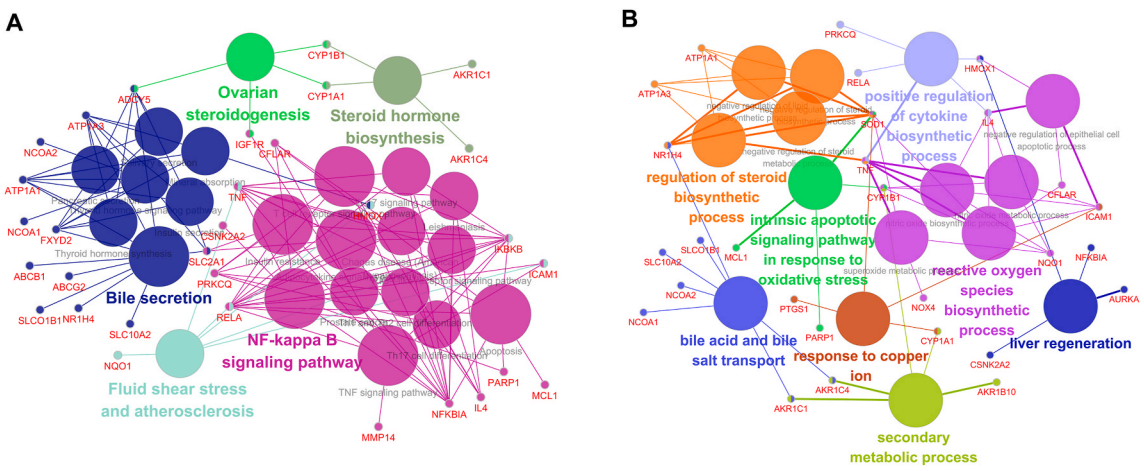

Fig. 3. Grouping of KEGG pathway enrichment (A) and GO biological process analysis (B) of CHI targets from XYLDF. The interaction between genes (targets) and terms was shown. A node represents a KEGG pathway or a GO biological process, and the node size is negatively correlated with the adjusted P-value of the pathway or biological process. Significant KEGG pathways and GO biological processes are classified into several functional groups based on κ value. The nodes of a group are labeled in the same color. Two groups share the nodes with two colors. Only the most significant term per group is shown with labels. (For interpretation of the references to color in this figure legend, the reader is referred to the Web version of this article.)

Table 2
KEGG Pathway enrichment analysis of XYLDF.

NO.	KEGG Pathway	PValue
1	Bile secretion	3.05E-12
2	NF-kappa B signaling pathway	1.62E-09
3	TNF signaling pathway	1.75E-06
4	Adipocytokine signaling pathway	1.85E-06
5	Apoptosis	9.02E-06
6	T cell receptor signaling pathway	1.92E-05
7	Insulin resistance	2.39E-05
8	Thyroid hormone signaling pathway	3.79E-05
9	Insulin secretion	9.72E-05
10	Fluid shear stress and atherosclerosis	1.17E-04

Table 3
GO biological process analysis of XYLDF.

NO.	GO Term	PValue
1	bile acid and bile salt transport	1.28E-11
2	reactive oxygen species biosynthetic process	5.39E-08
3	regulation of steroid biosynthetic process	3.23E-06
4	secondary metabolic process	3.82E-06
5	negative regulation of steroid biosynthetic process	3.59E-06
6	negative regulation of steroid metabolic process	4.47E-06
7	positive regulation of cytokine biosynthetic process	4.46E-06
8	response to copper ion	4.69E-06
9	nitric oxide biosynthetic process	5.51E-06
10	liver regeneration	6.49E-06

the NF-κB activation and NF-κB-mediated inflammation pathway.

4. Discussion

In this study, the main potential therapeutic targets of XYLDF predicted by network pharmacology, such as FXR, NF-κB, and TNF-α, were validated in the level of molecular biology. Moreover, our research indicated that XYLDF relieved cholestatic liver injury not only by modulating bile acid signaling pathway through FXR regulation, but also reducing inflammation response at the same time.

As a classical prescription of TCM, XYLDF is widely used for treating acute cholecystitis and cholangitis induced by hepatochlic hygropyrexia (Yin et al., 2008). Its liver-protective role on CHI has been confirmed in the previous research(Liu et al., 2016). The non-targeted metabolomics study revealed that the therapeutic effect of XYLDF was related to multiple metabolic pathways, including retinol metabolism, steroid hormone biosynthesis, pentose, and arachidonic acid metabolism, and especially for the primary bile acid biosynthesis pathway (Zhang et al., 2019), which is strongly interrelated with FXR signaling pathway in the literature (Chiang, 2013; Russell, 2003). Meanwhile, BAs-targeted metabolomics study showed recovery of the interrupted bile acid profile, as well as reduction of absolute contents of toxic bile acids in the liver of ANIT-induced cholestatic hepatic injury rats after oral administration of XYLDF (Zhang et al., 2019). In this study, the pharmacological mechanism of XYLDF on CHI was further explored and validated.

ANIT is a hepatotoxicant used in rodents to resemble human intrahepatic cholestasis, and ANIT-induced CHI is regarded as a useful model to study cholestatic hepatitis (Mehendale et al., 1994). The cholestasis induced by ANIT is characterized by necrosis of biliary epithelial cells

Table 4
Molecular docking energy of active compounds of XYLDF.

No.	Compound Name	Origin	Docking Energy(kcal/mol)			
			FXR	TNF	ICAM1	NF-κB
1	Andrographolide	CXL	−8.28	−5.03	−6.15	−7.07
2	Dehydroandrographolide	CXL	−8.22	−4.22	−4.9	−5.39
3	Apigenin-7-O-β-D-glucuronide	CXL	−6.35	−4.11	−5.52	−4.82
4	Nodosin	XHC	−8.79	−5.15	−5.78	−6.7
5	Enmein	XHC	−8.01	−5.56	−6.29	−7.21
6	Isodocarpin	XHC	−9.08	−5.86	−6.48	−7.4
7	4-methoxy-5-hydroxy-canthin-6-one	KM	−6.59	−5.19	−5.24	−5.28
8	1-methoxicabony-β-carboline	KM	−6.68	−4.91	−5.78	−5.52

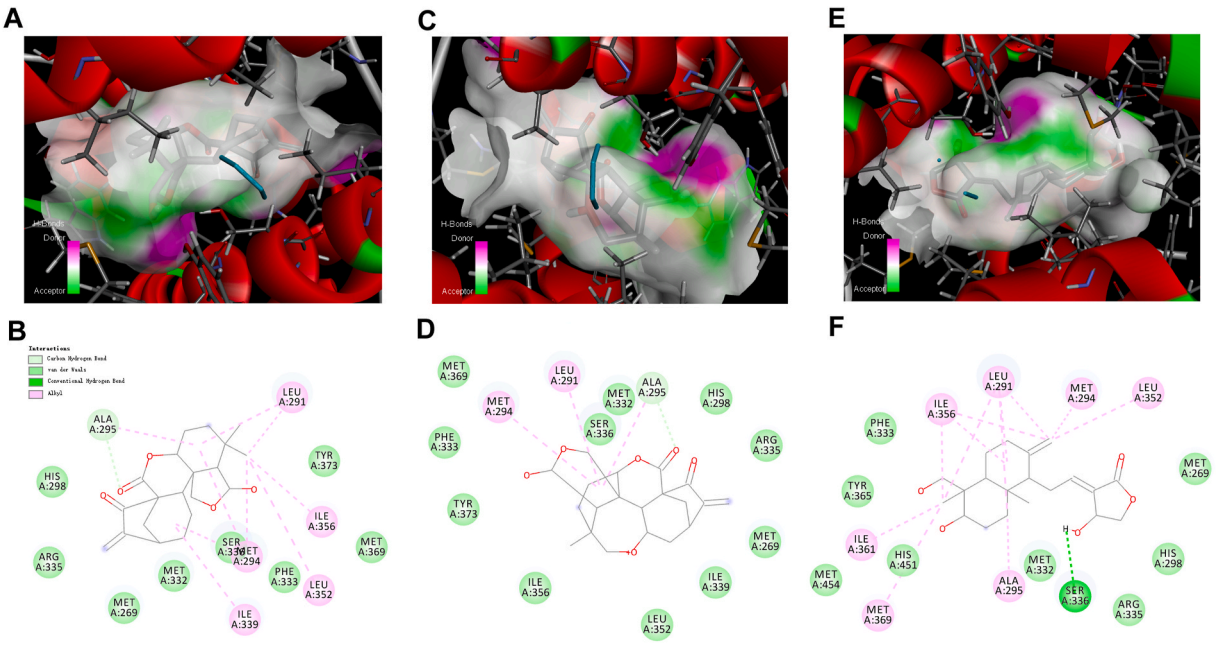

Fig. 4. The interactive modes of isodocarpin, nodosin and andrographolide with FXR. 3D graph showed that isodocarpin (A), nodosin (C), and andrographolide (E) were binding on the pocket of FXR protein. The electrical characteristics of the surrounding residues and the interaction between FXR and isodocarpin (B), nodosin (D), andrographolide (F) were visualized in 2D graph. The pink dotted line represented an alkyl hydrophobic bond, and the green dotted line represented a conventional hydrogen bond.(For interpretation of the references to colour in this figure legend, the reader is referred to the web version of this article.)

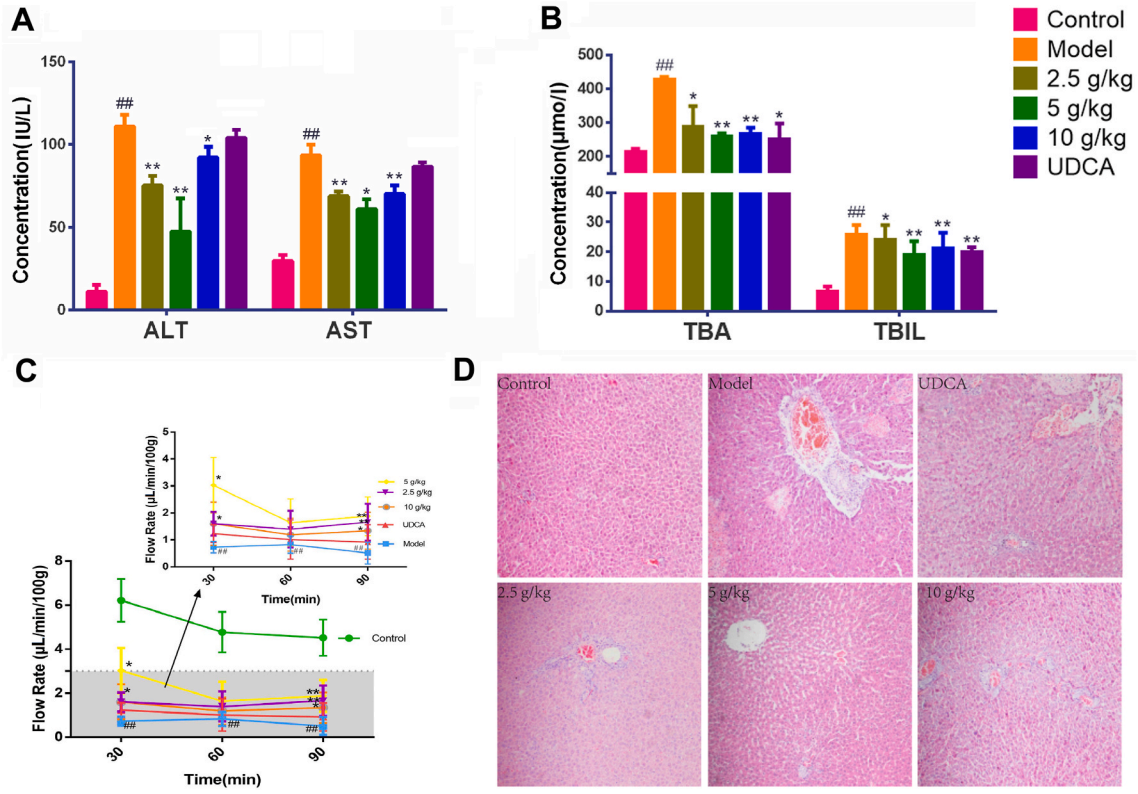

Fig. 5. Hepatoprotective effect of XYLDF against ANIT induced CHI in rats. Serum ALT and AST (A), TBA, and TBIL (B) levels were significantly reduced, Bile flow rate (C) increased. The liver pathologic was also improved (D) with the treatment of XYLDF of 5 g/kg. Bile flow rate, biochemical indicators, and liver pathologic in rats orally administered UDCA, 2.5, 5, or 10 g/kg of XYLDF, respectively, were determined at 48 h after soybean oil or ANIT administration. Data were presented as means ± SD (n = 8). $^{\#\#}p < 0.01$, $^{\#}p < 0.05$ compared with the control group, $^{**}p < 0.01$, $^{*}p < 0.05$ compared with the model group.

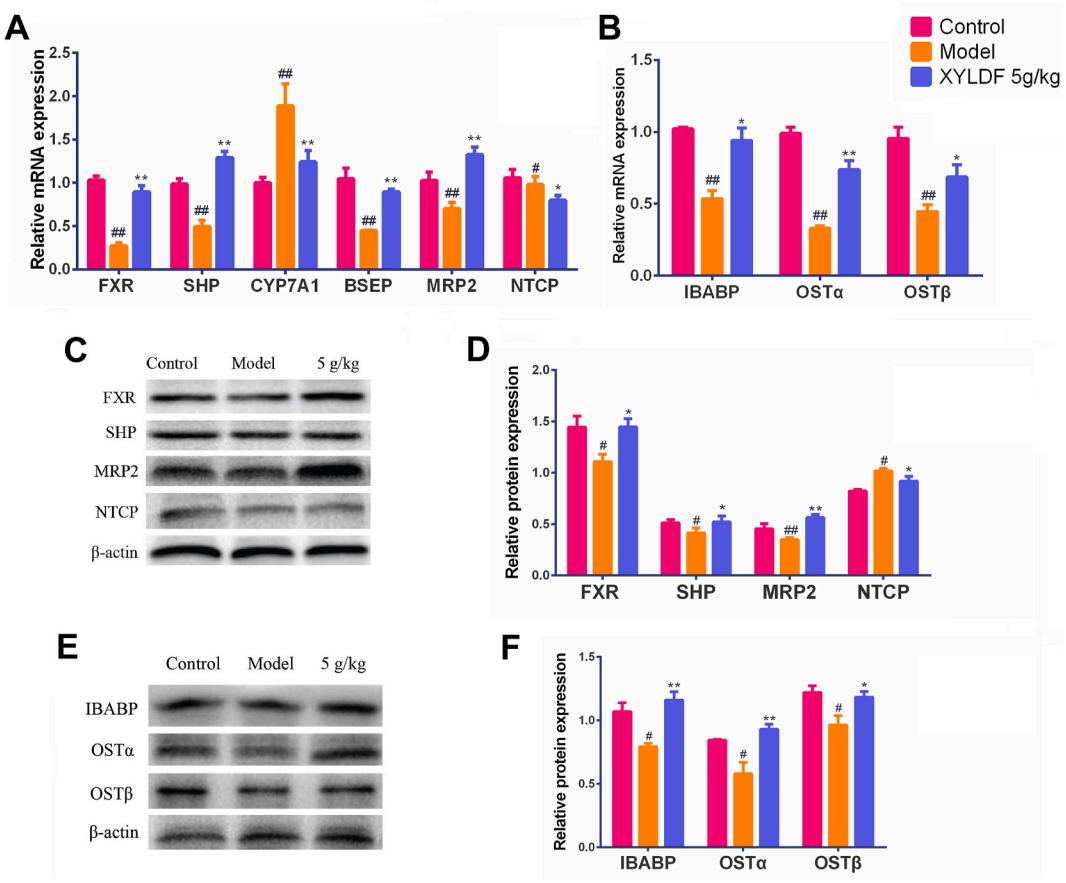

Fig. 6. XYLDF regulated the FXR-mediated bile acid pathway. XYLDF (5 g/kg) regulated liver mRNA (A) expression of FXR, SHP, CYP7A1, BSEP, MRP2, and NTCP involved in FXR pathway in ANIT-induced rat model. XYLDF also altered ileum mRNA (B) expression of IBABP, OSTα, and OSTβ in ANIT-induced rat model (n = 8). Protein level of liver FXR, SHP, MRP2, and NTCP (C), and ileum IBABP, OSTα, and OSTβ (E) were also regulated by XYLDF. The quantitative densitometric of proteins (D, F) were analyzed (n = 6). Data were presented as means ± SD. $^{\#\#}p < 0.01$, $^{\#} < < 0.05$ compared with the control group, $^{**}p < 0.01$, $^{*}p < 0.05$ compared with the model group.

and obstruction of bile ducts, which caused bile reflux and diffusion. The toxic bile acid further leads to the hepatocyte polarity loss and bile flow disruption, together with peripheral inflammation and hepatocyte injury(Wei et al., 2020). To investigate the effect of XYLDF on CHI and its mechanism, ANIT was selected to imitate the liver injury with bile acid circulation disorder caused by cholestasis. And the result suggested that XYLDF had a potential therapeutic impact on ANIT induced CHI in rats, which was manifested in the decrease of serum ALT, AST, TBA, and TBIL, the recovery of disrupted bile flow, and the improvement of pathological damage.

In the current study, the results of PPI network, KEGG pathway and GO functional enrichment analysis revealed that XYLDF mainly regulated FXR (NR1H4), bile acid and bile salt transportation, and bile secretion signaling pathway, which were all involved in CHI. As the core regulator of bile acid homeostasis, the nuclear receptor farnesoid X receptor (FXR) plays a significant role in physiological bile acid synthesis, secretion, and transportation (Cariello et al., 2018). Studies have revealed that defects of the FXR pathway accounted for the different clinical types of cholestasis (Wagner et al., 2009), and promoting FXR activation performed an excellent curative effect in CHI (Zhao et al., 2019; Marin et al., 2015). In our study, FXR was decreased by ANIT, which was consistent with the previous findings (Wang et al., 2017), and the up-regulated expression after the XYLDF treatment suggesting the protective effect of XYLDF against ANIT-induced CHI by stimulating the expression of FXR. Moreover, it has been proven that FXR inhibits synthesis and uptake of bile acids in the liver through SHP activation to stimulate the bile acid detoxification pathway (Karimian et al., 2013). As revealed by the data of our research, FXR was significantly activated after XYLDF treatment. It also promoted the expression of the downstream gene, SHP, which directly restrained the expression of CYP7A1, the first rate-limited enzyme of bile acid synthesis, to reduce the production of bile acids and its toxicity. The results suggested that restraint of bile acid synthesis might be one of the mechanisms of XYLDF to relieve bile acid accumulation. Moreover, the regulation of XYLDF on primary bile acid biosynthesis confirmed in our previous metabolomics study was also approved in this part (Zhang et al., 2019). Additionally, bile acids have their maintenance in the enterohepatic circulation under physiological conditions. Abnormal expression and function of transporters and enzymes of bile acids would cause hepatic accumulation of bile acids and further aggravate liver damage (Xu et al., 2017; Soroka and Boyer, 2014). Studies have reported that regulating bile acid transporters, such as MRP2 and BSEP, protects against ANIT-induced CHI (zhang et al., 2016; Chen et al., 2016; Zhao et al., 2017). Our experimental results demonstrated that XYLDF significantly increased the hepatic expression of MRP2 and BSEP to increase the efflux of bile acids. Meanwhile, the gene expression of NTCP was down-regulated by XYLDF, which reminded the reabsorption of bile acids into the liver was restrained, thereby limiting the increase of hepatic bile acid levels (Massafra et al., 2018). Moreover, evidence showed that inhibition of intestinal bile acid absorption protected against bile acid-mediated cholestatic liver disease (Baghdasaryan et al., 2016). In our study, the iliac bile acid transporters, IBABP and OSTα/β were elevated in both mRNA and protein levels, which manifested that both the reabsorption and efflux of bile acids in ileum were promoted.

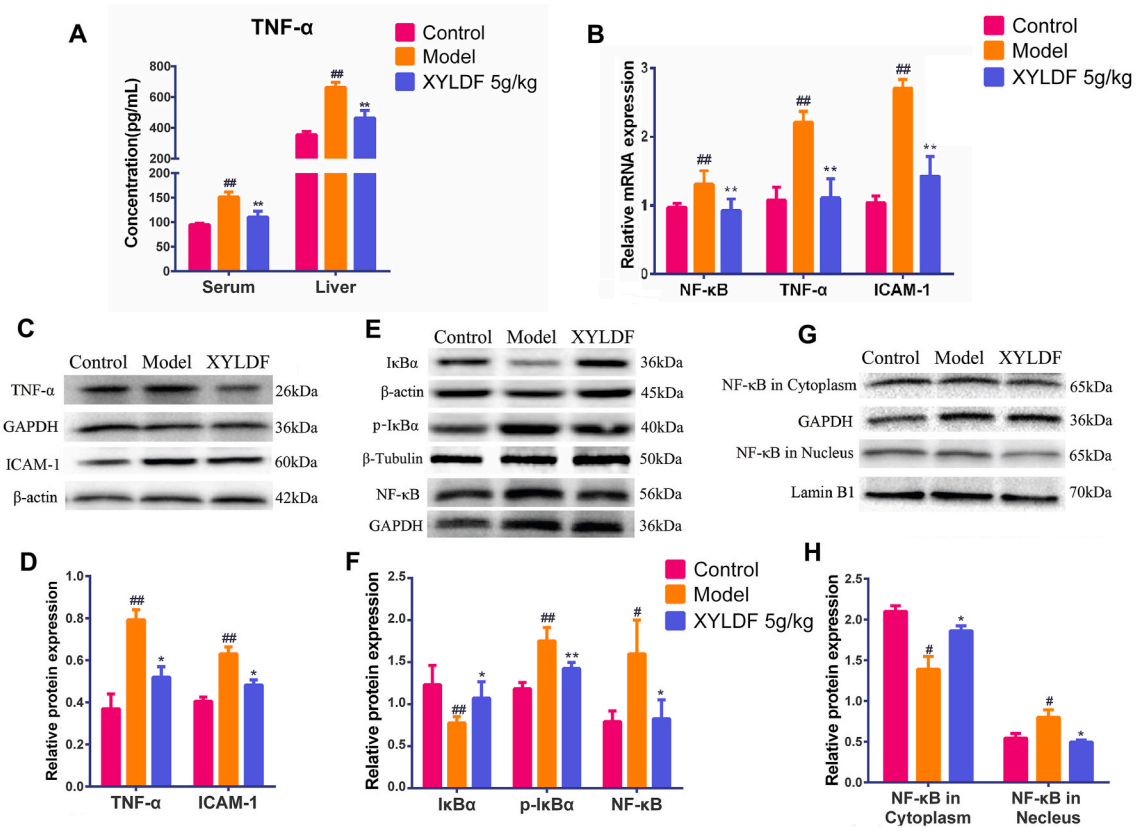

Fig. 7. XYLDF reduced inflammation and inhibited NF-κB nuclear translocation. XYLDF reduced the levels of TNF-α in plasma and liver (A) (n = 8). The liver mRNA (B) expression involved in inflammation including NF-κB, TNF-α, and ICAM-1were suppressed in the XYLDF group (n = 8).And the protein level of TNF-α and ICAM-1had the similar trend (C, D)as mRNA expression (n = 6). Meanwhile, protein level of NF-κB, IκBα, p-IκBα, NF-κB in the cytoplasm and nucleus (E-H) were altered (n = 6) by XYLDF. Data were presented as means ± SD. $^{\#\#}p < 0.01$, $^{\#}p < 0.05$ compared with the control group, $^{**}p < 0.01$, $^{*}p < 0.05$ compared with the model group.

Taken together, XYLDF depressed the intrahepatic bile acid level and relieved CHI by regulating bile acid synthesis, secretion, and transportation. Notably, it has been proven that the two vital transporters, MRP2 and BSEP, are targeted gene of FXR and directly induced by FXR at transcriptional level (Chen et al., 2013; Cai and Boyer, 2006), and FXR also induces IBABP and OSTα/β expression (Dawson et al., 2005) and negatively regulates NTCP expression (Neimark et al., 2004). Therefore, it can be indicated that XYLDF promoted bile acid transportation and reduced bile acid synthesis and reabsorption, and that process was highly correlated with the activating of FXR signaling pathway.

According to the PPI network analysis, inflammatory factors, including NF-κB, TNF-α, and ICAM-1, were highlighted as putative targets. KEGG pathway enrichment result reasoned NF-κB signaling pathway as another important mechanism of XYLDF on CHI. As the inflammatory response results in acquired dysfunction of hepatocytes, current opinions believe that inflammation is one of the crucial reasons for the injury caused by cholestasis (Donepudi et al., 2012). In this study, a hepatic injury was induced by ANIT with strong signs of inflammation response occurred, which could be reflected with the activation of NF-κB signaling pathway and an enhancement of TNF-α, and ICAM-1 in plasma and liver tissue. That confirms previously reported facts (Fang et al., 2017; Ma et al., 2018). NF-κB acts as a core mediator in inflammatory responses, its activation induces a series of inflammatory cytokines primarily related to TNF-α and ICAM-1 in hepatocytes (Jin et al., 2013). In an inactive state, NF-κB is inhibited by IκBα according to masking the nuclear localization signals of NF-κB proteins and keeping them sequestered in the cytoplasm. And The activation of NF-κB requires the phosphorylation of IκBα by the IκB kinase complex and the subsequent degradation of IκBα. In our study, the phosphorylation of IκBα was suppressed (Fig. 7E and F), and the nuclear translocation of NF-κB was inhibited (Fig. 7G and H) in XYLDF group, which results in the inhibition of pro-inflammatory cytokine expression and release, including TNF-α and ICAM-1 (Fig. 7A–C). It suggested that the inflammatory response in hepatocytes was relieved. The above findings supported that XYLDF had an effect of inhibiting NF-κB activation in cholestatic hepatic injury and repressed inflammation.

In CHI, cholestasis happens followed with bile flow disruption, and leads to the accumulation of bile acids and other bile components, the hepatobiliary toxicity finally results in liver injury (Cui et al., 2009). Consistent reports showed that overload hepatic bile acids could directly induce the inflammatory responses and trigger the hepatocyte necrosis (Yuan and Li, 2016), and the relief of cholestatic hepatic injury was usually accompanied by a reduction of hepatic bile acids (Wang et al., 2017). Our previous study exhibited that XYLDF reduced the accumulation of hepatic toxic bile acid after ANIT treatment. On the basis of interactions between bile acid and inflammatory, it seems reasonable that the regulation of bile acid synthesis and transportation was the pivotal mechanism of XYLDF on the treatment of CHI. Besides, activation of FXR was reported to reduce inflammation, antagonize the NF-kB signaling pathway, and inhibit the expression of inflammatory cytokines (Wang et al., 2008), and FXR-deficient could lead to NF-κB activation (Wu et al., 2015). Thereby, as XYLDF regulated bile acid metabolism to alleviate hepatic cholestasis, and then exhibited an anti-inflammatory effect simultaneously in the treatment of the hepatic injury, it can be speculate that XYLDF repressed the CHI by modulating FXR and NF-κB activation, which demonstrated the treatment character of multiple targets in the TCM formula.

5. Conclusions

The current study applied a combined method of network pharmacology with animal experimental validation to explore the hepatoprotective mechanism of XYLDF against CHI. The prediction from network pharmacology suggested the mechanism of XYLDF for CHI was mainly referred to FXR-mediated bile acid signaling pathway and NF-κB-mediated pro-inflammatory signaling pathway. The results of our subsequent animal experiments strongly supported the prediction by regulating the ANIT-induced abnormal expression of enzymes and transporters of BAs related to enterohepatic circulation, and cytokines correlated to hepatic inflammation, tended to the levels of control group after XYLDF treatment in rats. The present research explored the mechanism of XYLDF for the treatment of CHI at a molecular level and supplied further evidence for the clinical use of it.

Declaration of competing interest

All authors declare no conflicts of interest.

Acknowledgments

The project was financially supported by grants from the National Natural Science Foundation of China (No. 81974520, 81873091, 81673872, 81773969, 81173535), and the grants form Major Research Projects for the Traditional Chinese Medicine Discipline of Guangzhou of CM (2020–2022).

Appendix A. Supplementary data

Supplementary data to this article can be found online at https://doi.org/10.1016/j.jep.2021.113816.

Author contributions

C.L. and C.Z. conceived and designed the experiments; M.W., R.Z. and F.L. performed the experiments; Y.Y., Q.Z, and Z.L analyzed the data; C.Z. contributed reagents/materials; M.W. and C.L. wrote the manuscript. All authors reviewed the manuscript and approved its submission.

References

Baghdasaryan, A., Fuchs, C.D., Österreicher, C.H., Lemberger, U.J., Halilbasic, E., Påhlman, I., Graffner, H., Krones, E., Fickert, P., Wahlström, A., Ståhlman, M., Paumgartner, G., Marschall, H.U., Trauner, M., 2016. Inhibition of intestinal bile acid absorption improves cholestatic liver and bile duct injury in a mouse model of sclerosing cholangitis. J. Hepatol. https://doi.org/10.1016/j.jhep.2015.10.024.

Banerjee, S., Bhattacharjee, P., Kar, A., Mukherjee, P.K., 2019. LC–MS/MS analysis and network pharmacology of Trigonella foenum-graecum – a plant from Ayurveda against hyperlipidemia and hyperglycemia with combination synergy. Phytomedicine 60. https://doi.org/10.1016/j.phymed.2019.152944.

Cai, S.Y., Boyer, J.L., 2006. FXR: a target for cholestatic syndromes? Expert Opin. Ther. Targets. https://doi.org/10.1517/14728222.10.3.409.

Carbone, M., Neuberger, J.M., 2014. Autoimmune liver disease, autoimmunity and liver transplantation. J. Hepatol. https://doi.org/10.1016/j.jhep.2013.09.020.

Cariello, M., Piccinin, E., Garcia-Irigoyen, O., Sabbà, C., Moschetta, A., 2018. Nuclear receptor FXR, bile acids and liver damage: introducing the progressive familial intrahepatic cholestasis with FXR mutations. Biochim. Biophys. Acta (BBA) - Mol. Basis Dis. https://doi.org/10.1016/j.bbadis.2017.09.019.

Chávez-Talavera, O., Tailleux, A., Lefebvre, P., Staels, B., 2017. Bile acid control of metabolism and inflammation in obesity, type 2 diabetes, dyslipidemia, and nonalcoholic fatty liver disease. Gastroenterology. https://doi.org/10.1053/j.gastro.2017.01.055.

Chen, Y., Song, X., Valanejad, L., Vasilenko, A., More, V., Qiu, X., Chen, W., Lai, Y., Slitt, A., Stoner, M., Yan, B., Deng, R., 2013. Bile salt export pump is dysregulated with altered farnesoid X receptor isoform expression in patients with hepatocellular carcinoma. Hepatology. https://doi.org/10.1002/hep.26187.

Chen, H., Huang, X., Min, J., Li, W., Zhang, R., Zhao, W., Liu, C., Yi, L., Mi, S., Wang, N., Wang, Q., Zhu, C., 2016. Geniposidic acid protected against ANIT-induced hepatotoxity and acute intrahepatic cholestasis, due to Fxr-mediated regulation of Bsep and Mrp2. J. Ethnopharmacol. https://doi.org/10.1016/j.jep.2015.12.033.

Chen, Qi, Zhang, Boli, 2016. Methodology for Pharmacodynamic Research in Traditional Chinese Medicine. People's Medical Publishing House.

Chiang, J.Y.L., 2013. Bile acid metabolism and signaling. Comp. Physiol. https://doi.org/10.1002/cphy.c120023.

Chinese Pharmacopoeia Commission, 2020. Pharmacopoeia of the People's Republic of China, I. China Medical Science and Technology Press, Beijing.

Crocenzi, F.A., Sánchez Pozzi, E.J., Pellegrino, J.M., Favre, C.O., Rodríguez Garay, E.A., Mottino, A.D., Coleman, R., Roma, M.G., 2001. Beneficial effects of silymarin on estrogen-induced cholestasis in the rat: a study in vivo and in isolated hepatocyte couplets. Hepatology. https://doi.org/10.1053/jhep.2001.26520.

Cui, Y.J., Aleksunes, L.M., Tanaka, Y., Goedken, M.J., Klaassen, C.D., 2009. Compensatory induction of liver efflux transporters in response to ANIT-induced liver injury is impaired in FXR-Null mice. Toxicol. Sci. https://doi.org/10.1093/toxsci/kfp094.

Dawson, P.A., Hubbert, M., Haywood, J., Craddock, A.L., Zerangue, N., Christian, W.V., Ballatori, N., 2005. The heteromeric organic solute transporter α-β, Ostα-Ostβ, is an ileal basolateral bile acid transporter. J. Biol. Chem. https://doi.org/10.1074/jbc.M412752200.

Donepudi, A.C., Aleksunes, L.M., Driscoll, M.V., Seeram, N.P., Slitt, A.L., 2012. The traditional ayurvedic medicine, Eugenia jambolana (Jamun fruit), decreases liver inflammation, injury and fibrosis during cholestasis. Liver Int. https://doi.org/10.1111/j.1478-3231.2011.02724.x.

El Kasmi, K.C., Vue, P.M., Anderson, A.L., Devereaux, M.W., Ghosh, S., Balasubramaniyan, N., Fillon, S.A., Dahrenmoeller, C., Allawzi, A., Woods, C., McKenna, S., Wright, C.J., Johnson, L., D'Alessandro, A., Reisz, J.A., Nozik-Grayck, E., Suchy, F.J., Sokol, R.J., 2018. Macrophage-derived IL-1β/NF-κB signaling mediates parenteral nutrition-associated cholestasis. Nat. Commun. 9 https://doi.org/10.1038/s41467-018-03764-1.

Fang, Z.Z., Tanaka, N., Lu, D., Jiang, C.T., Zhang, W.H., Zhang, C., Du, Z., Fu, Z.W., Gao, P., Cao, Y.F., Sun, H.Z., Zhu, Z.T., Cai, Y., Krausz, K.W., Yao, Z., Gonzalez, F.J., 2017. Role of the lipid-regulated NF-κB/IL-6/STAT3 axis in alpha-naphthyl isothiocyanate-induced liver injury. Arch. Toxicol. https://doi.org/10.1007/s00204-016-1877-6.

Fickert, P., Pollheimer, M.J., Silbert, D., Moustafa, T., Halilbasic, E., Krones, E., Durchschein, F., Thüringer, A., Zollner, G., Denk, H., Trauner, M., 2013. Differential effects of norUDCA and UDCA in obstructive cholestasis in mice. J. Hepatol. https://doi.org/10.1016/j.jhep.2013.01.026.

Hirschfield, G.M., Chapman, R.W., Karlsen, T.H., Lammert, F., Lazaridis, K.N., Mason, A.L., 2013. The genetics of complex cholestatic disorders. Gastroenterology. https://doi.org/10.1053/j.gastro.2013.03.053.

Jin, F., Cheng, D., Tao, J.Y., Zhang, S.L., Pang, R., Guo, Y.J., Ye, P., Dong, J.H., Zhao, L., 2013. Anti-inflammatory and anti-oxidative effects of corilagin in a rat model of acute cholestasis. BMC Gastroenterol. https://doi.org/10.1186/1471-230X-13-79.

Karimian, G., Buist-Homan, M., Schmidt, M., Tietge, U.J.F., de Boer, J.F., Klappe, K., Kok, J.W., Combettes, L., Tordjmann, T., Faber, K.N., Moshage, H., 2013. Sphingosine kinase-1 inhibition protects primary rat hepatocytes against bile salt-induced apoptosis. Biochim. Biophys. Acta (BBA) - Mol. Basis Dis. https://doi.org/10.1016/j.bbadis.2013.06.011.

Li, M., Cai, S.Y., Boyer, J.L., 2017. Mechanisms of bile acid mediated inflammation in the liver. Mol. Aspect. Med. https://doi.org/10.1016/j.mam.2017.06.001.

Liang, X., Li, H., Li, S., 2014. A novel network pharmacology approach to analyse traditional herbal formulae: the Liu-Wei-Di-Huang pill as a case study. Mol. Biosyst. https://doi.org/10.1039/c3mb70507b.

Liu, A.L., Du, G.H., 2010. Network pharmacology: new guidelines for drug discovery. Acta Pharm. Sin.

Liu, F., Lin, C., Zhao, Wei, Zhu, C., 2016. The intervention effect of Xiaoyan Lidan tablets on ANIT-induced intrahepatic cholestasis rats. J. Chin. Med. Mater. 39, 898–901.

Ma, X., Wen, J.X., Gao, S.J., He, X., Li, P.Y., Yang, Y.X., Wei, S.Z., Zhao, Y.L., Xiao, X.H., 2018. Paeonia lactiflora Pall. regulates the NF-κB-NLRP3 inflammasome pathway to alleviate cholestasis in rats. J. Pharm. Pharmacol. https://doi.org/10.1111/jphp.13008.

Marin, J.J.G., Macias, R.I.R., Briz, O., Banales, J.M., Monte, M.J., 2015. Bile acids in physiology, pathology and pharmacology. Curr. Drug Metabol. https://doi.org/10.2174/1389200216666151103115454.

Martincuks, Antons, Andryka, Katarzyna, Küster, Andrea, Schmitz-Van de Leur, Hildegard, Komorowski, Michal, Müller-Newen, Gerhard, 2017. Nuclear translocation of STAT3 and NF-κB are independent of each other but NF-κB supports expression and activation of STAT3. Cell. Signal. https://doi.org/10.1016/j.cellsig.2017.01.006.

Massafra, V., Pellicciari, R., Gioiello, A., van Mil, S.W.C., 2018. Progress and challenges of selective Farnesoid X Receptor modulation. Pharmacol. Ther. https://doi.org/10.1016/j.pharmthera.2018.06.009.

Mehendale, H.M., Roth, R.A., Gandolfi, A.J., Klaunig, J.E., Lemasters, J.J., Curtis, L.R., 1994. Novel mechanisms in chemically induced hepatotoxicity 1. Faseb. J. https://doi.org/10.1096/fasebj.8.15.8001741.

Meng, Q., Chen, X.L., Wang, C.Y., Liu, Q., Sun, H.J., Sun, P.Y., Huo, X.K., Liu, Z.H., Yao, J.H., Liu, K.X., 2015. Alisol B 23-acetate protects against ANIT-induced hepatotoxity and cholestasis, due to FXR-mediated regulation of transporters and enzymes involved in bile acid homeostasis. Toxicol. Appl. Pharmacol. https://doi.org/10.1016/j.taap.2015.01.020.

Mohi-Ud-Din, R., Lewis, J.H., 2004. Drug- and chemical-induced cholestasis. Clin. Liver Dis. https://doi.org/10.1016/S1089-3261(03)00124-7.

Neimark, E., Chen, F., Li, X., Shneider, B.L., 2004. Bile acid-induced negative feedback regulation of the human ileal bile acid transporter. Hepatology. https://doi.org/10.1002/hep.20295.

Ou, Q.Q., Qian, X.H., Li, D.Y., Zhang, Y.X., Pei, X.N., Chen, J.W., Yu, L., 2016. Yinzhihuang attenuates ANIT-induced intrahepatic cholestasis in rats through upregulation of Mrp2 and Bsep expressions. Pediatr. Res. https://doi.org/10.1038/pr.2015.252.

Palmeira, C.M., Ferreira, F.M., Rolo, A.P., Oliveira, P.J., Santos, M.S., Moreno, A.J., Cipriano, M.A., Martins, M.I., Seiça, R., 2003. Histological changes and impairment of liver mitochondrial bioenergetics after long-term treatment with α-naphthyl-isothiocyanate (ANIT). Toxicology. https://doi.org/10.1016/S0300-483X(03)00163-X.

Russell, D.W., 2003. The enzymes, regulation, and genetics of bile acid synthesis. Annu. Rev. Biochem. https://doi.org/10.1146/annurev.biochem.72.121801.161712.

Shen, B., Yin, H., Zhu, X.P., Xiao, W.X., Zhou, J., Xiao, G.Y., Zhou, H.J., 2018. Laparoscopic cholecystectomy combined with Xiaoyanlidan tablets for treatment of acute cholecystitis patients: curative effect and impact on prognosis and serological indicators. World Chin. J. Dig. https://doi.org/10.11569/wcjd.v26.i25.1523.

Soroka, C.J., Boyer, J.L., 2014. Biosynthesis and trafficking of the bile salt export pump, BSEP: therapeutic implications of BSEP mutations. Mol. Aspect. Med. https://doi.org/10.1016/j.mam.2013.05.001.

Tang, D.Q., Li, Z., Jiang, X.L., Li, Y.J., Du, Q., Yang, D.Z., 2014. Fingerprint analysis and multi-ingredient quantitative analysis for quality evaluation of Xiaoyanlidan tablets by ultra high performance liquid chromatography with diode array detection. J. Separ. Sci. https://doi.org/10.1002/jssc.201400362.

Wagner, M., Zollner, G., Trauner, M., 2009. New molecular insights into the mechanisms of cholestasis. J. Hepatol. https://doi.org/10.1016/j.jhep.2009.05.012.

Wang, Y.D., Chen, W.D., Wang, M., Yu, D., Forman, B.M., Huang, W., 2008. Farnesoid X receptor antagonizes nuclear factor κB in hepatic inflammatory response. Hepatology. https://doi.org/10.1002/hep.22519.

Wang, H., Fang, Z.Z., Meng, R., Cao, Y.F., Tanaka, N., Krausz, K.W., Gonzalez, F.J., 2017. Glycyrrhizin and glycyrrhetinic acid inhibits alpha-naphthyl isothiocyanate-induced liver injury and bile acid cycle disruption. Toxicology. https://doi.org/10.1016/j.tox.2017.05.012.

Wang, L., Wu, G., Wu, F., Jiang, N., Lin, Y., 2017. Geniposide attenuates ANIT-induced cholestasis through regulation of transporters and enzymes involved in bile acids homeostasis in rats. J. Ethnopharmacol. https://doi.org/10.1016/j.jep.2016.12.022.

Wei, X., Fan, X., Feng, Z., Ma, Y., Lan, X., Chen, M., 2020. Ethyl acetate extract of herpetospermum pedunculosum alleviates α-naphthylisothiocyanate-induced cholestasis by activating the farnesoid x receptor and suppressing oxidative stress and inflammation in rats. Phytomedicine. https://doi.org/10.1016/j.phymed.2020.153257.

Wu, W. Bin, Chen, Y.Y., Zhu, B., Peng, X.M., Zhang, S.W., Zhou, M.L., 2015. Excessive bile acid activated NF-kappa B and promoted the development of alcoholic steatohepatitis in farnesoid X receptor deficient mice. Biochimie. https://doi.org/10.1016/j.biochi.2015.05.014.

Xu, L., Sheng, T., Liu, X., Zhang, T., Wang, Z., Han, H., 2017. Analyzing the hepatoprotective effect of the Swertia cincta Burkillextract against ANIT-induced cholestasis in rats by modulating the expression of transporters and metabolic enzymes. J. Ethnopharmacol. https://doi.org/10.1016/j.jep.2017.07.031.

Yang, N., Xiong, A., Wang, R., Yang, L., Wang, Z., 2016. Quality evaluation of traditional Chinese medicine compounds in xiaoyan lidan tablets: fingerprint and quantitative analysis using UPLC-MS. Molecules. https://doi.org/10.3390/molecules21020083.

Yin, X.P., Li, Y.B., B, L., 2008. Effects of xiaoyanlidanpian on experimental hepatitis and acute inflammation. Chinese J. Exp. Tradit. Med. formula 14, 45–48.

Yuan, Z.Q., Li, K.W., 2016. Role of farnesoid X receptor in cholestasis. J. Dig. Dis. https://doi.org/10.1111/1751-2980.12378.

Zhang, B., Lu, C., Bai, M., He, X., Tan, Y., Bian, Y., Xiao, C., Zhang, G., Lu, A., Li, S., 2015. Tetramethylpyrazine identified by a network pharmacology approach ameliorates methotrexate-induced oxidative organ injury. J. Ethnopharmacol. https://doi.org/10.1016/j.jep.2015.09.034.

zhang, A., Jia, Y., Xu, Q., Wang, C., Liu, Q., Meng, Q., Peng, J., Sun, H., Sun, P., Huo, X., Liu, K., 2016. Dioscin protects against ANIT-induced cholestasis via regulating Oatps, Mrp2 and Bsep expression in rats. Toxicol. Appl. Pharmacol. https://doi.org/10.1016/j.taap.2016.06.019.

Zhang, Y., Huang, X., Zhou, J., Yin, Y., Zhang, T., Chen, D., 2018. PPARγ provides anti-inflammatory and protective effects in intrahepatic cholestasis of pregnancy through NF-κB pathway. Biochem. Biophys. Res. Commun. 504, 834–842. https://doi.org/10.1016/j.bbrc.2018.09.035.

Zhang, R., Huang, T., Zhang, Q., Yao, Y., Liu, C., Lin, C., Zhu, C., 2019. Xiaoyan lidan formula ameliorates α-naphthylisothiocyanate-induced intrahepatic cholestatic liver injury in rats as revealed by non-targeted and targeted metabolomics. J. Pharmaceut. Biomed. Anal. https://doi.org/10.1016/j.jpba.2019.112966.

Zhang, Z., Miao, Y., Xu, M., Cheng, W., Yang, C., She, X., Geng, Q., Zhang, Q., 2019. TianJiu therapy for α-naphthyl isothiocyanate-induced intrahepatic cholestasis in rats treated with fresh Ranunculus sceleratus L. J. Ethnopharmacol. https://doi.org/10.1016/j.jep.2019.112310.

Zhao, Y., Ma, X., Wang, J., Wen, R., Jia, L., Zhu, Y., Li, R., Wang, R., Li, J., Wang, L., Li, Y., Xiao, X., 2015. Large dose means significant effect - dose and effect relationship of Chi-Dan-Tui-Huang decoction on alpha-naphthylisothiocyanate-induced cholestatic hepatitis in rats. BMC Compl. Alternative Med. https://doi.org/10.1186/s12906-015-0637-0.

Zhao, Y., He, X., Ma, X., Wen, J., Li, P., Wang, J., Li, R., Zhu, Y., Wei, S., Li, H., Zhou, X., Li, K., Liu, H., Xiao, X., 2017. Paeoniflorin ameliorates cholestasis via regulating hepatic transporters and suppressing inflammation in ANIT-fed rats. Biomed. Pharmacother. https://doi.org/10.1016/j.biopha.2017.02.025.

Zhao, Q., Liu, F., Cheng, Y., Xiao, X.R., Hu, D.D., Tang, Y.M., Bao, W.M., Yang, J.H., Jiang, T., Hu, J.P., Gonzalez, F.J., Li, F., 2019. Celastrol protects from cholestatic liver injury through modulation of SIRT1-FXR signaling. Mol. Cell. Proteomics. https://doi.org/10.1074/mcp.RA118.000817.

Zhu, G., Feng, F., 2019. UHPLC-MS-based metabonomic analysis of intervention effects of Da-Huang-Xiao-Shi decoction on ANIT-induced cholestasis. J. Ethnopharmacol. https://doi.org/10.1016/j.jep.2019.111860.